

Estimation of the Local Scour from a Cylindrical Bridge Pier Using a Compilation Wavelet Model and Artificial Neural Network

Mehran Seifollahi ¹
Mohammad Ali Lotfollahi-Yaghin ²
Farhoud Kalateh ²

Rasoul Daneshfaraz ³
Salim Abbasi ⁴
John P. Abraham ⁵

Abstract

In the present study, an artificial neural network and its combination with wavelet theory are used as the computational tool to predict the depth of local scouring from the bridge pier. The five variables measured are the pier diameter of the bridge, the critical and the average velocities, the average diameter of the bed aggregates, and the flow depth. In this study, the neural wavelet method is used as a preprocessor. The data was passed through the wavelet filter and then passed to the artificial neural network. Among the various wavelet functions used for preprocessing, the *dmey* function results in the highest correlation coefficient and the lowest RMSE and is more efficient than other functions. In the wavelet-neural network compilation method, the neural network activator function was replaced by different wavelet functions. The results show that the neural network method with the *Polywog4* wavelet activator function with a correlation coefficient of 87% is an improvement of 8.75% compared to the normal neural network model. By performing data filtering by wavelet and using the resulting coefficients in the neural network, the resulting correlation coefficient is 82%, only a 2.5% improvement compared to the normal neural network. By analyzing the results obtained from neural network methods, the wavelet-neural network predicted errors compared to experimental observations were 8.26, 1.56, and 1.24%, respectively. According to the evaluation criteria, combination of the best effective hydraulic parameters, the combination of wavelet function and neural network and the number of neural network neurons achieved the best results.

Keywords: Artificial Neural Network, Bridge Cylindrical Pier, Scour Depth, Wavelet Theory.

Received: 03 September 2021; Accepted: 02 November 2021

¹ Faculty of Civil Engineering, University of Tabriz, Tabriz, Iran. E-mail: m.seifollahi94@yahoo.com
(Corresponding Author)

² Faculty of Civil Engineering, University of Tabriz, Tabriz, Iran.

³ Department of Civil Engineering, University of Maragheh, Maragheh, Iran.

⁴ Department of Civil Engineering, University of Mohaghegh Ardabili, Ardabil, Iran.

⁵ School of Engineering, University of St. Thomas, St Paul, MN, USA.

1. Introduction

The cause of most destruction to bridges is erosion around the bridge piers. This occurs due to the complex eddy vortices and the formation of horseshoe flow and scouring in front of the piers. Experimental-analytical relationships have been created based on the experimental data. Most of the proposed empirical relationships consider the final scour depth as a function of flow characteristics such as average velocity at the bridge pier, flow depth, fluid characteristics, particle density, mean bed particle diameter, fluid viscosity, and other parameters.

Data mining is an analytical process that validates data using patterns. Artificial neural networks (ANNs), as one of the main branches of these systems, are made of simple operating elements that work in parallel together. These elements are inspired by biological nervous systems (the human brain). These networks are a type of computational model that can determine the relationship between the inputs and outputs of a system by a network of nodes that are all interconnected.

The concept of the wavelet was first introduced in the early 1980s. Wavelets are used as a tool in mathematics, physics, digital signal processing, computer vision, numerical calculations, audio and video information compression, geophysics, etc. Generally, applying a mathematical conversion to a signal is a way to obtain additional information that is not available in the original raw signal. In most processing approaches in various engineering sciences, the primary raw signal is the desired signal in the time domain. From a scientific point of view, if a mathematical or physical variable has rapid changes, it is called "high frequency", and conversely, if the signal changes are slow, the signal is called "low frequency". Frequency indicates the rate of change of the corresponding variable.

Firat and Gungor [1] used a neural network model to predict scour depth and showed that the neural network model has acceptable performance. Pier diameter and medium particle size have the greatest effect on the scouring of non-stick soils. Guven et al. [2] used genetic programming to estimate scouring around cylindrical piers and concluded that genetic programming can estimate scour depth better than neural fuzzy inference systems and regression equations. Azamathulla et al. [3] used neural networks and genetic programming to estimate scouring around a bridge pier. They showed that genetic programming is more accurate than neural networks and regression equations. Toth and Brandimarte [4] predicted the depth of scouring from bridge piers in clear water and living bed conditions by comparing experimental relationships with an artificial neural network. Scattering and mean absolute error values showed that neural network models usually provide the best performance of scour depth estimation. Mostaghimzadeh et al. [5] studied the accuracy of prediction-based reservoir exploitation policy using discrete wavelet transform and group learning methods. The results showed that the performance of the feature selection model in identifying the variables affecting the monthly flow over the monthly flow is appropriate and identifying four effective features with a relative error of 0.31 identifies the pattern of flow changes. Karimae Tabarestani and Zarrati [6] studied the design of riprap around bridge piers using experimental methods and artificial neural networks. In order to achieve higher accuracy for riprap design, they developed the artificial neural network (ANN) method based on the use of dimensionless parameters. Najafzadeh et al. [7] presented relationships for estimating scour depth using artificial neural networks using the numerical classification of group data (GMDH).

Chen et al. [8]; Postalcioglu and Becerikli [9]; Mayorga et al. [10]; Zhong and Song [11]; Nazaruddin [12]; In their research, Fang and Chow [13], used tidal forecasting in the South China Sea, modeling of nonlinear systems, applications in approximate signals, runoff forecasting, vehicle suspension, and performance approximation forecasting, respectively.

Roshangar et al. [14] used the fuzzy neural method and support vector machine to predict scour depth. The results of that study showed that the output of ANFIS is most consistent with the experimental data. Sarshari and Mullhaupt [15] estimated the depth of a scour pit downstream of a bridge pier. The selection of the type of network with a certain number of neurons was accomplished by trial and error, and finally, the neural network with 5 neurons in the hidden layer showed the best performance. Bonakdari and Ebtehaj [16] used an adaptation neural fuzzy system and neural network to estimate scour depth. They compared the output of the two models with the output of the nonlinear regression method. The results of this study showed that the neural network compared to ANFIS provides a more accurate result and is closer to the output from a nonlinear regression method. Esmaeili-Varaki et al. [17] investigated scouring around bridge piers using intelligent methods such as fuzzy-neural adaptation systems optimized with genetic algorithms and neural networks. This study showed that the fuzzy system optimized by the algorithm with a correlation coefficient of 99% and a mean error of 0.024 has a better performance than the neural network method. Ismail [18] presented an empirical relation based on an evolutionary regression network to predict the depth of scouring around bridge piers. Comparison with existing models showed that the proposed relationship model produces an accurate and reasonable estimate of the scour equilibrium depth with a much smaller number of suitable constants compared to Back-Propagation neural networks. Sreedhara et al. [19] used hybrid soft-computing algorithms to optimize support vector particle swarm optimization, and artificial neural network-based fuzzy inference systems (PSO-SVM) to predict scour depth around a pier with different shapes. The results showed that the PSO-SVM model is an accurate and efficient method for predicting scour depth.

Sadeghfam et al. [20] studied the scouring for supercritical current jets upstream of lattice plates in experiments using artificial intelligence methods. In that research, Sugeno fuzzy logic (SFL), neuro-fuzzy (NF) and support vector machine (SVM) methods were used. Daneshfaraz et al. [21] investigated the effects of cables on local scouring of bridge piers in the experimental and ANN and ANFIS algorithms. Comparisons showed that the ANN method (C.C = 0.9843) has considerable accuracy compared to the ANFIS method (C.C = 0.7626). Ashrafi et al. [22] used the discrete wavelet transform and artificial neural networks to predict the monthly inflow of the Dez reservoir. The results showed that if the results prediction scheme is presented accurately, the predicted operating law curves are superior to ordinary rules. Daneshfaraz et al. [23] used SVM method to predict the effect of screens diameter on hydraulic parameters of vertical drop. The results showed that changing the diameter of the screens had no effect on energy dissipation and the output data from SVM had the best agreement with the laboratory data. Ghoshchi et al. [24] predicted the output of the wind power plant's using weather and power plant parameters and the extended Fuzzy Wavelet Neural Network (FWNN), and also developed an effective model for short-term wind power forecasting. The results showed that compared to other previously reported methods, the proposed method was a more efficient performance and had higher accuracy for short-term forecast of wind power. Anshuka et al. [25] calculated different drought indices for areas around Fiji and conducted a correlation study using two satellite vegetation products: Normalized Difference Vegetation Index and Enhanced vegetation index. In this study, an artificial neural network model transformed into a WANN wavelet) was used to generate short-term predictions. The important point was that due to the repetitive nature of the forecast, the model could be updated and improved with more data available.

Ouma et al. [26] compared the LSTM and WNN wavelet neural network methods for Spatio-temporal rainfall prediction and measured runoff time-series trends in hydrological basins. The

results showed that in hydrological basins with sparse meteorological and hydrological monitoring networks, the use of satellite meteorological data in deep learning neural network models is suitable for spatial and temporal analysis of rainfall and runoff trends. Rady [27] used two methods of artificial intelligence modeling, namely genetic programming (GP) and ANFIS, to predict the depth of pier scouring. Evaluation criteria showed that the GP approach provides more accurate results when compared to the ANFIS model or any other empirical equation. Siahkali et al. [28] conducted research to investigate how alternative models of scour depth around circular piers are estimated and they compared the results with experimental formulas. The results show that the estimations from the Gaussian process are more accurate than the experimental equations. Daneshfaraz et al. [29] examined the performance of the support vector machine on the hydraulic parameters of a vertical drop equipped with a dual screen; they concluded that the residual relative energy yields $RMSE= 0.0056$ and $R^2= 0.994$ and for the relative downstream depth, $RMSE= 0.0064$ and $R^2= 0.986$. Fuladipanah and Majediasl [30] used the support vector machine algorithm and field data from the US Geological Survey to analyze two scenarios. The scouring depth from a bridge pier was predicted based on different combinations of dimensionless parameters. Comparison of the results showed that the SVM algorithm estimated the scour values more accurately than the observed values with an absolute error between 11 and 35%. Norouzi et al. [31] predicted the relative energy dissipation parameters in a vertical slope equipped with horizontal screen using soft computation techniques. The results showed that the output data from soft calculations have a very good agreement with laboratory data.

Based on the studies conducted in the field of scouring, it is obvious that the scouring depth depends on several parameters. Given the complexity of the interaction of these factors with each other, the development of a model to examine the relationship between effective parameters and the performing a sensitivity analysis of parameters seems necessary. Intelligent methods that are able to predict the depth of scouring at a bridge pier can lead to significant savings in computational costs and analysis time. In previous studies, wavelet transforms have not been used to estimate the depth of local scour. In the present study, the combination of wavelet and artificial neural network, a kind of multivariate regression, has been used. The main purpose of this research, in the first step, is to use fast wavelet transform methods and artificial neural networks and to introduce an efficient method that provides the least acceptable error. In the next step, the initial and reliable way to estimate the scour depth by changing the geometric and hydraulic parameters is reviewed. Also, soft computational models with different analysis processes are proposed, which are finally compared with other soft calculation methods.

2. Materials and methods

2.1. Wavelet Theory

The main focus is on displacement rather than on instantaneous rates of change. Different wavelets, the scale functions of which can be seen in Table 5, have been used. Based on previous studies, three methods have been proposed to calculate the instantaneous frequency: 1. The Marseille method, which uses the continuous wavelet transform phase to estimate the dominant instantaneous frequency; 2. The Carmona method; and 3. the Simple method. The first two methods are mostly used for signals that have noise; the third, simple method, has been used to estimate the instantaneous frequency. In the simple method, a wavelet transform is first taken from the signal and at each time step, the frequency with the highest amplitude is considered the dominant instantaneous frequency.

Figure 1 shows some sets of wavelets in the time domain. These sets are classified into discrete and continuous types.

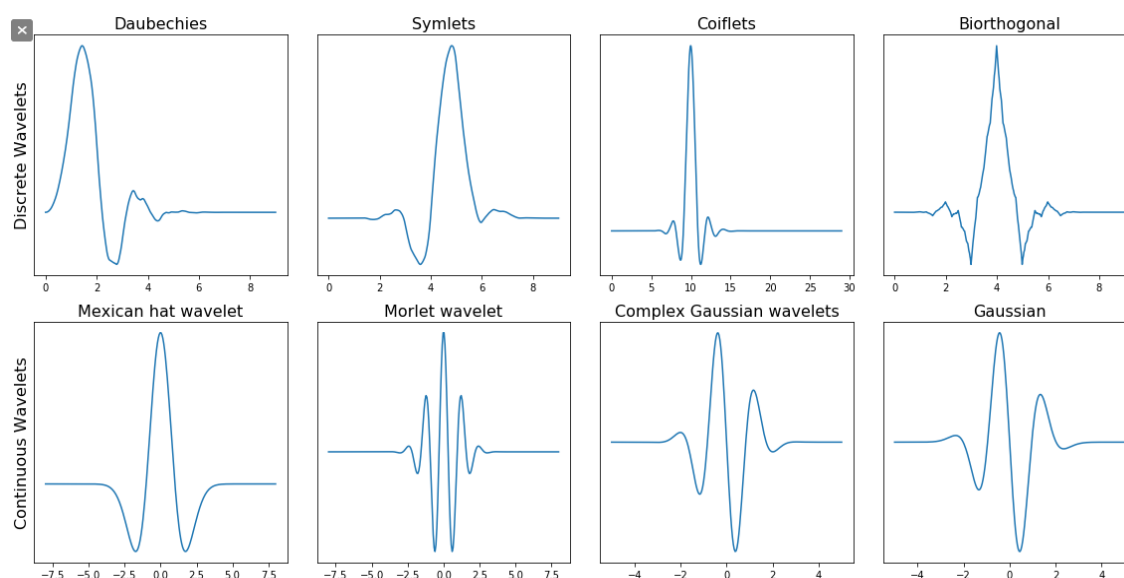


Figure 1. Different wavelets in the time domain [32]

For a signal at level n to be decomposable, the main signal must have a minimum length of $2n$. The advantage of using this method in signal decomposition is that the conversion of frequency and time is performed simultaneously and there are no restrictions on Fourier frequency conversion. Discrete wavelet transforms are more useful than continuous data because the data converted by this method have no additional components and can be converted to data types in the time or frequency domains.

2.2. Theory of wavelet combination and artificial neural network

Neural network activating functions must be continuous and defined in the range -1 to 1 . Wavelet functions that have these properties can be substituted for the activator function. As shown in Figure 1, all functions have the features mentioned. Wavelet transformations and the neural network form a mapping network called the wavelet-neural network. As a special case, feed neural networks are proposed to approximate observable variables. Approaches based on wavelet-based artificial neural networks can be divided into two main groups: In the first group, the wavelet section is separated from the network training section and has a separate information processing relative to each other. Thus, neural network structures are formed based on wavelet analysis. This model actually separates the input parameters into small and general components by the wavelet and provides these components as input to the neural network. This method introduces a per-network signal analysis filter. One of the important advantages of these filters is their ability to detect regular components that occur in irregular input parameters [33]. Discrete wavelet transforms have been used in this research because they require fewer calculations than their continuous counterparts. When both wavelets and neural networks are combined in a single

technique, instantaneous error approximations are reduced using special algorithms. The wavelet functions are entered only as activating functions in the neural network estimation process and the transmission coefficients and the wavelet scale remain constant. Figure 2 shows a schematic of the presented wavelet network (wavenet) models.

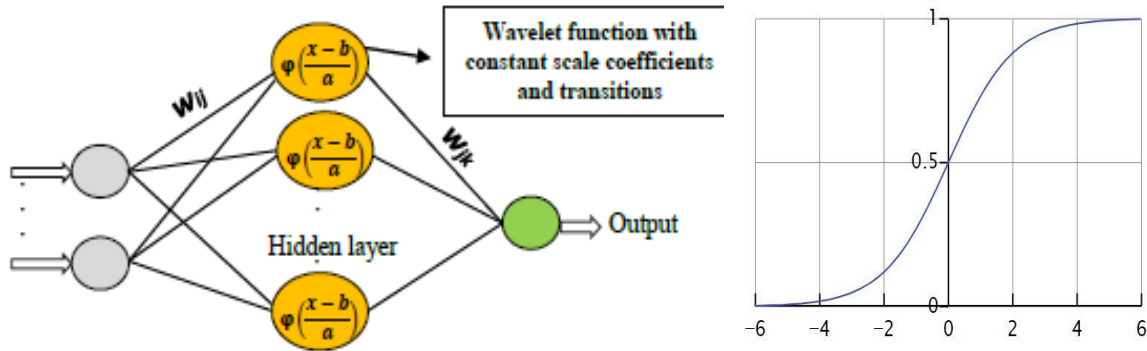


Figure 2. Wavenet schematic structure and schematic of the sigmoid activation function [12]

2.3. Scour Depth Prediction Equations and Evaluation Criteria

Table 1 presents equations used to estimate scour depth. In these relationships, most of the variables that express the characteristics of the river or bridge piers are used and are obtained cross-sectionally. These relationships are obtained using dimensional analysis and are presented in a dimensionless manner. These relationships estimate the amount of scouring with acceptable accuracy.

Table 1. Equations presented by previous researchers to estimate scour depth

Researcher	Equations presented
Coleman [34]	$\frac{V}{\sqrt{2gd_s}} = 0.6 \left(\frac{V}{\sqrt{gb}} \right)^{0.9}$
Norman [35]	$d_s = 3.b^{0.3}$
Jain and Fischer [36]	$\frac{d_s}{b} = 1.41 \left(\frac{y}{b} \right)^{0.3} \left(\frac{V_c}{\sqrt{gy}} \right)^{0.25}$
Esmaeili-Varaki et al. [17]	$\frac{d_s}{D_*} = f \left(\frac{y}{D_*}, \frac{U}{U_c}, \frac{z}{D_*}, \frac{t}{t_e}, Fr \right)$
Samaga et al. [37]	$\frac{d_s}{y} = 4.0.y_1.y_2.y_3.y_4 \left(\frac{V}{gy} \right)^n$
Guynakti [38]	$\frac{d_s}{b} = 1.183 \left(\frac{y}{b} \right)^{0.471}$
Melville & Suthurland [39]	$\frac{d_s}{b} = k_i.k_y.k_d.k_\sigma.k_s.k_\alpha$
U.S. DOT. [40]	$\frac{d_s}{Y} = K_3 \left(\frac{Y}{D} \right)^{-0.65} \left(\frac{U}{\sqrt{gY}} \right)^{0.43}$
Melville and Coleman [41]	$d_s = k_{yb}.k_l.k_s.k_d.k_\theta.k_G.k_t$

To evaluate the capability of networks, the statistical parameters of root mean square error (RMSE) and correlation coefficient (R) are calculated using the following relations:

$$RMSE = \sqrt{\frac{\sum_{k=1}^N (t_k - y_k)^2}{N}} \quad (1)$$

$$R = \frac{\sum_{k=1}^N (t_k - \bar{t}_k)(y_k - \bar{y}_k)}{\sqrt{\sum_{k=1}^N (t_k - \bar{t}_k)^2 \sum_{k=1}^N (y_k - \bar{y}_k)^2}} \quad (2)$$

In these relationships, t_k is the target output, y_k is the output of the network, (\bar{t}_k) is the average targetoutput, and N is the number of training pairs. The model with the lowest RMSE values and the highest R value (closest to 1) is selected as the best model [42].

3. Database Bank

The data used to train and validate the network are the results of several sets of experiments, compiled and presented by the University of Sydney, Australia [43]. The data include 190 case studies compiled by the University of Sydney, Australia. Table 2 lists the names of the researchers and the number of physical models that were tested by the respective researchers.

Table 2. Number of results of the data series tested by previous researchers

Row	Researcher	Number of physical models tested
1	Kothyari et al. [44]	72
2	Melville and Raudkivi [45]	13
3	Chabert and Engeldinger [46]	6
4	Chee [47]	3
5	Cheiw [48]	14
6	Ettema [49]	15
7	Graf [50]	3
8	Hancu [51]	2
9	Jain and Fischer [36]	4
10	Jeng et al. [43]	1
11	Kwan [52]	1
12	Melville [53]	12
13	Oliveto and Hager [54]	44

This data is presented in the form of a matrix, each column of which represents a parameter. According to Table 3, the input matrix consists of five columns named d_{50} , D , U , b and U_c , which represent the average diameter of the bed sediment, pier diameter, average flow velocity, flow depth, and critical flow velocity, respectively, and the output matrix. It consists of a row representing the local scour depth of the bridge pier (ds).

Table 3. Effective parameters defined in the input and output matrices

Row	Input matrix	Output matrix
1	Medium bed sediment (d_{50})	
2	Pier diameter (D)	
3	Average flow velocity (U)	pier local scour depth (d_s)
4	Flow depth (b)	
5	Critical flow velocity (U_c)	

Figure 3 shows the changes of each of the aforementioned parameters. Out of 190 experimental measurement series available, 144 were randomly selected and used for network training. According to Figure 3, the rate of change of the critical velocity is higher while the changes in the depth of flow are less. The vertical axis of Figure 3 shows the parameters limit, and the horizontal axis shows experimental case item numbers. This figure aims to show all parameters limit per item.

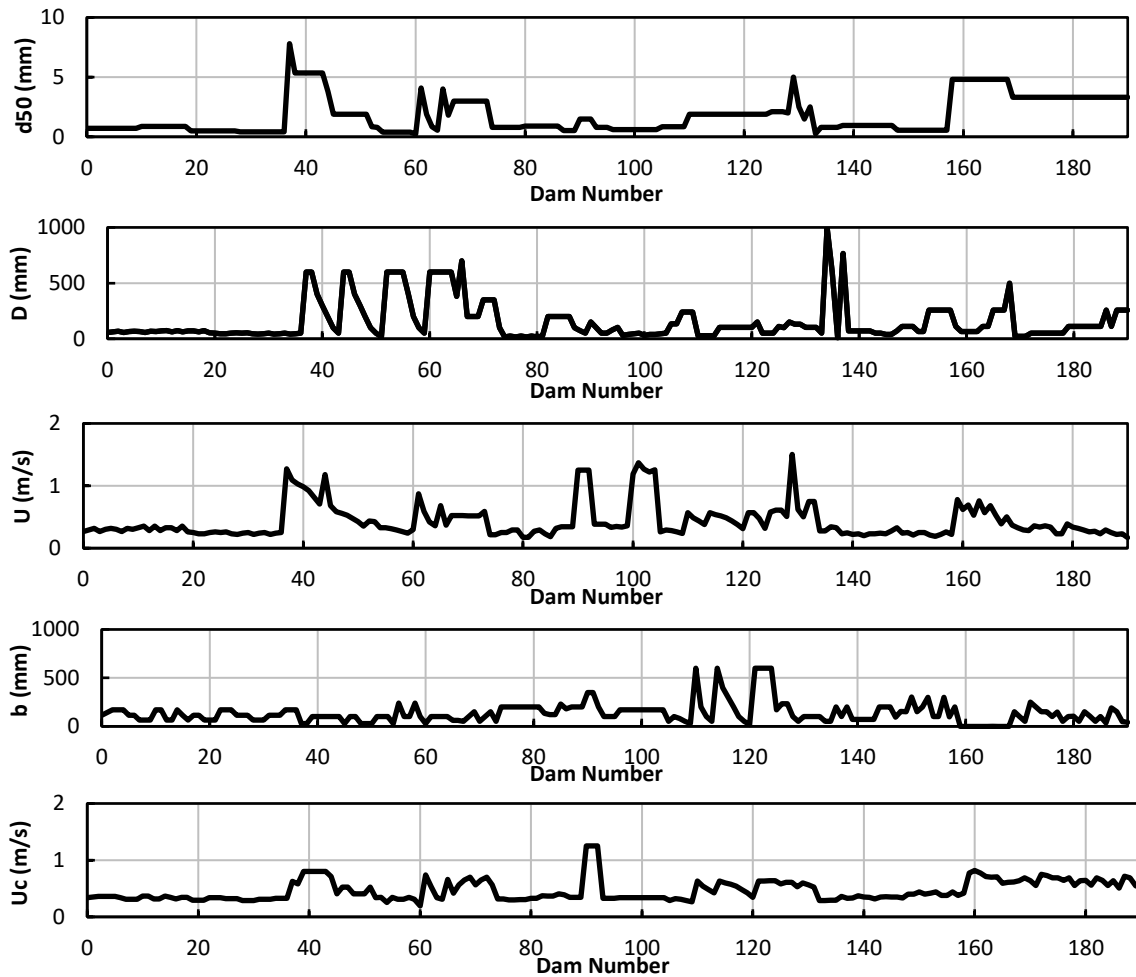


Figure 3. Chart of variables used



4. Discussion and Results

4.1. Results from the Artificial Neural Network Model

In the artificial neural network model, by maintaining the network structure, learning law, and other effective factors, the network was trained to use transmission functions. The results of training and validation of the neural network model with two evaluation criteria are presented in Table 4. The neural network with 11 neurons provided the best performance and the results from the statistical analysis are listed in the table. For this purpose, a single-layer network with 10 intermediate nodes (10 computational neurons) and gradient reduction Back-Propagation learning law (BPGD) was used.

Minimal error was obtained when the sigmoid transfer function was used. To achieve optimal education, the network was trained up to 100 repetitions steps. The results show that the smallest error occurs when the Levenberh-Margaret (LM) Back-Propagation law is applied. The output of the sigmoid stimulus function used in the Reverse Propagation algorithm is in the range between zero and one, so the output value of the training pairs should be in the same range. All stages of analysis have been repeated several times to obtain accurate values. Of the total data, 144 datapoints were used for training and 46 for random prediction. The mapping operation was performed using the following general rule (Equation 3):

$$x_i = \frac{X_i - X_{i \min}}{X_{i \max} - X_{i \min}} \quad (3)$$

As x_i represents the mapped values of the inputs X_i , $X_{i \max}$, and $X_{i \min}$ are the maximum and minimum values in the range x_i , respectively. The number of hidden layer nodes is also an important parameter of the back-propagation network. The network training rate and the number of network repetitions are considered to be 0.1 and 100, respectively, and with increasing root mean square error, the network training process is automatically stopped. Figures 4 and 5 show the overlap of all adaptive data and the total data error for this model, respectively. Figure 6 shows the distribution of the ratio of exact values to predicted values.

Table 4. Results from the neural network model

Number of neurons	R		RMSE	
	Train	Test	Train	Test
11	0.8115	0.8005	0.1890	0.1882

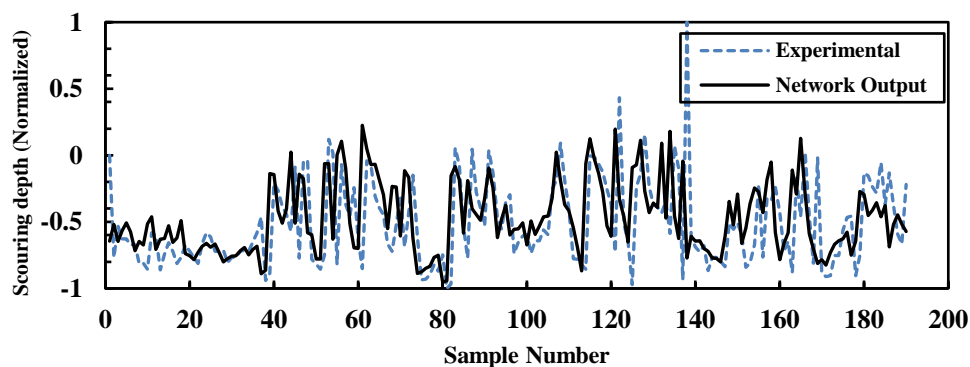


Figure 4. Overlap of experimental data and results predicted by the artificial neural network for the full dataset

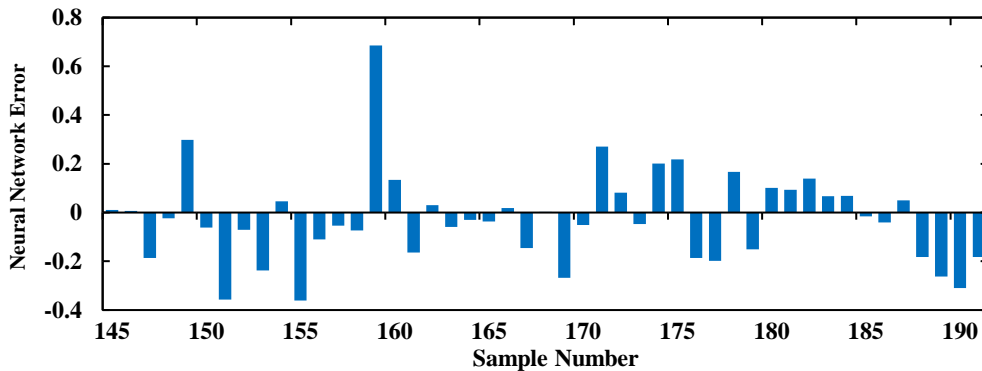


Figure 5. Artificial neural network prediction error values for the full dataset

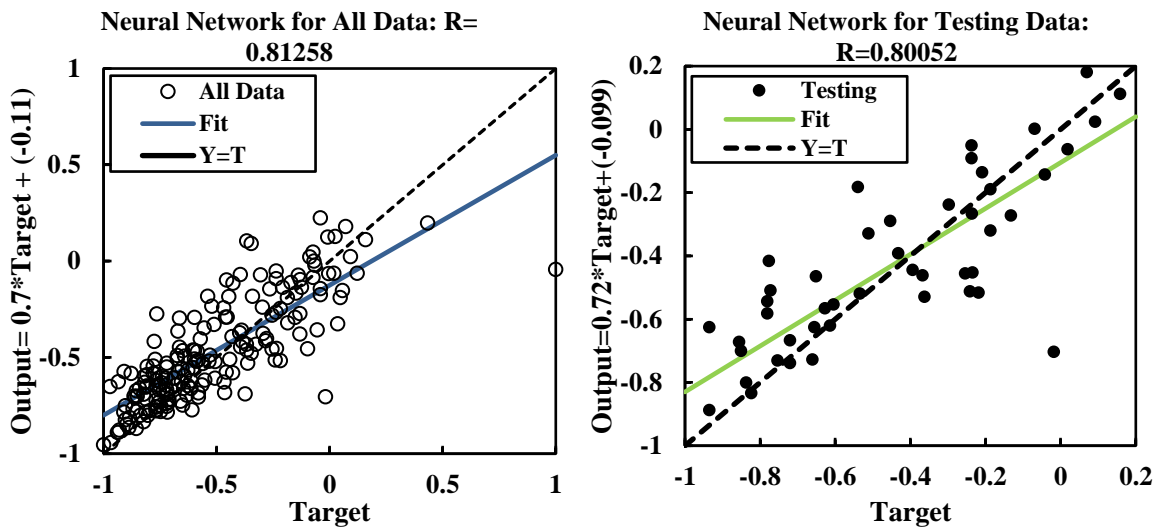


Figure 6. Correlation coefficient representation for validation data in the artificial neural network model

From Figures 4, 5, and 6, the performance of the neural network method for estimating scour depth can be examined. Figure 4 shows the overlap and comparison of predictions with experimental measurements. By analyzing the data in Figure 4, the error in predictions of the final scouring depth from the neural network method was determined to be 8.26%.

Figure 5 shows the resulting error for the final result. The accuracy limits along with the minimum and maximum range are extracted and compared. Figure 6 shows the deviation from the 100% prediction and how it is distributed throughout the data. In this figure, the estimated data are plotted against the corresponding laboratory data, so that if the estimate is perfect, all points are on the 1:1 line.



Table 5. Comparison of the results of previous studies and the present study using the ANN model

researcher	Previous research used in ANN	RMSE	MAPE	CC	R ²	MAE
Choi & Cheong [55]	Laursen and Toch [56]	–	179.15	–	–	–
	Neill [57]	–	272.33	–	–	–
	Jain and Fischer [36]	–	436.65	–	–	–
	CSU [55]	–	165.39	–	–	–
	Melville [53]	–	264.98	–	–	–
Lee et al. [58]	Laursen and Toch [56]	1.0138	–	0.8160	–	–
	Shen [59]	0.5994	–	0.7119	–	–
	Hancu [51]	1.1360	–	0.7303	–	–
	Coleman [34]	0.4765	–	0.6786	–	–
	Ettema et al. [60]	1.5825	–	0.7523	–	–
	BPN [58]	0.1393	–	0.9559	–	–
Batani et al. [61]	Laursen and Toch [56]	0.0727	–	–	0.5288	0.0497
	Shen [59]	0.0640	–	–	0.5815	0.0444
	Hancu [51]	0.1188	–	–	0.3284	0.0720
	Breusers et al. [62]	0.1039	–	–	0.1221	0.0613
	Melville and Sutherland [39]	0.1326	–	–	0.5350	0.0761
	Melville [53]	0.0589	–	–	0.6000	0.0411
	Melville and Chiew [63]	0.0519	–	–	0.6074	0.0393
	ANN (MLP/BP) [61]	0.0078	–	–	0.9879	0.0051
ANN (RBF/OLS) [61]	0.0251	–	–	0.8422	0.0180	
Ismail et al. [64]	Melville and Chiew [63]	0.21914	–	–	0.6020	–
	Laursen and Toch [56]	0.21295	–	–	0.5195	–
	Shen [59]	0.20828	–	–	0.4604	–
	HEC-18 US DoT [40]	0.20065	–	–	0.5943	–
	GRNN [64]	0.13876	–	–	0.7240	–

researcher	Previous research used in ANN	RMSE	MAPE	CC	R ²	MAE
	Sigmoid network [64]	0.10570	–	–	0.8366	–
	Optimised network [64]	0.09301	–	–	0.8725	–
	Salim and Jones [66]	1.4970	–	–	0.366	1.120
	HEC-18 US DoT [40]	1.0640	–	–	0.726	0.770
Zounemat-Kermani et al. [65]	Sheppard and Glasser [67]	0.9910	–	–	0.818	0.697
	Ataie-Ashtiani and Beheshti [68]	0.8210	–	–	0.866	0.649
	FFBP-NN (Zounemat-Kermani et al. [65])	0.3900	–	–	0.966	0.270
	RBF-NN (Zounemat-Kermani et al. [65])	0.5300	–	–	0.936	0.370
Present Study	ANN	0.1882	–	–	0.8005	–

According to the performance criteria set forth in Table 5, the RMSE and R² criteria are the most commonly used statistical metrics. By comparing RMSE and R² criteria in the study of Bateni et al. [61], with 98% accuracy, Ismail et al. [64], estimated scour depth around a bridge pier with 83% accuracy. The present study, with 80% accuracy, had the highest efficiency. The neural networks used examined more data, and in fact, due to the wider information community and more experimental variables, better results were obtained than the neural networks mentioned. As shown in Table 5, while many studies have been performed to estimate scour depth, the previous research is limited to the ANN method; there is a lack of investigation using the wavelet approach. The present work is unique in that it utilizes both of these techniques together.

4.2. Results of Combining a Wavelet Model and ANN

Wavelet transform, which is a tool for converting signals from the time domain to frequency, was used to separate the data changes on a case-by-case basis. Therefore, by decomposing the neural network into harmonic signals, it improved the results. With the combined model using both wavelets and an artificial neural network, wavelet transforms were used as a data preprocessor to separate all 5 input variables into several subsets at different levels. Neural network uncertainty is within an acceptable range that can be calculated and determined using different methods; interested readers are invited to Farokhnia and Morid [69], Khashei et al. [70], Lan et al. [71], and Pourreza Bilondi and Khashei-Siuki [72], Table 6 presents the numerical results of criteria considered for evaluating the efficiency of models. The first column of Table 6 deals with wavelet functions selected as preprocessors. The wavelet coefficients obtained from the conversion of variables include two approximate subsets (D) and general (A) [73]. Several combinations of each of these subsets were studied.

Table 6. Evaluation criteria values for wavelet model and artificial neural network

Wavelet	Number of neurons	of (Combination - Surface) Separation	R		RMSE	
			Train	Test	Train	Test
sym4	24	4 - D	0.69	0.69	0.258	0.219
coif4	23	3 - D	0.65	0.80	0.288	0.175
db4	23	4 - A, D	0.72	0.77	0.232	0.197
rbio6.8	23	3 - A, D	0.77	0.77	0.234	0.228
dmey	22	3 - A, D	0.85	0.82	0.179	0.182
haar	23	2 - A, D	0.75	0.78	0.233	0.205
bior6.8	18	3 - D	0.84	0.81	0.175	0.185

According to the numerical results related to Table 6, among the different wavelet functions used, the *dmey* function has the highest correlation coefficient and the lowest RMSE. The *dmey* function provides better performance than other functions and modes. The main reason for this excellent performance is the adaptation of the wavelet function to different parts of the input variables because the *dmey* wavelet function moves symmetrically and faster to zero than other wavelet functions. Therefore, it is more accurate in analyzing and separating the signal in question than other wavelet functions. The reason for choosing the optimal wavelet function is not just to consider one criterion, but to consider all the criteria together and at the same time, and also the difference and the effect of the performance criterion is important. Figure 7, shows the mother wavelet diagram *dmey* showing zero convergence in the range $x = (6, -6)$.

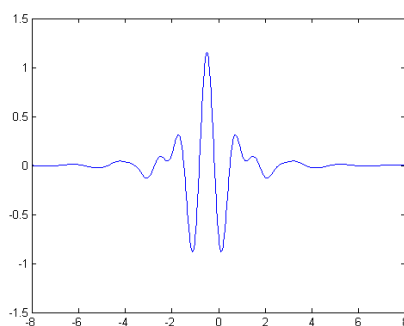
**Figure 7. the shape of the *dmey* wavelet function**

Figure 8 shows the overlap of experimental data and output of the wavelet and neural network combination model for total dataset. In addition to the error value, the amount of the error, more or less than the actual value, can be seen. By analyzing the results of Figure 8, the error in predicting the final scour depth of the *dmey* wavelet and neural network combination method compared with laboratory observations was 1.56%.

Figure 10 shows the distribution of the ratio of exact values to predicted values. In the figure, the estimated data are punctuated against the corresponding experimental data. If the estimates were perfect, all points would lie on the 1:1 line.

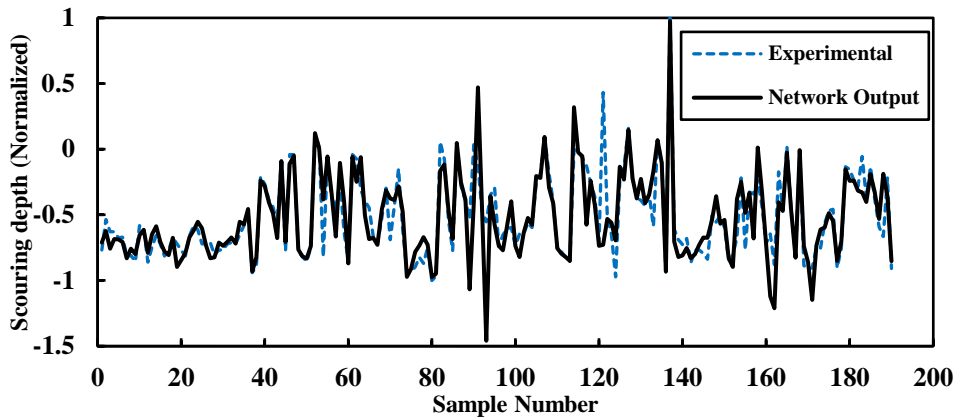


Figure 8. Overlap of results from wavelet neural network and experimental data for the total dataset

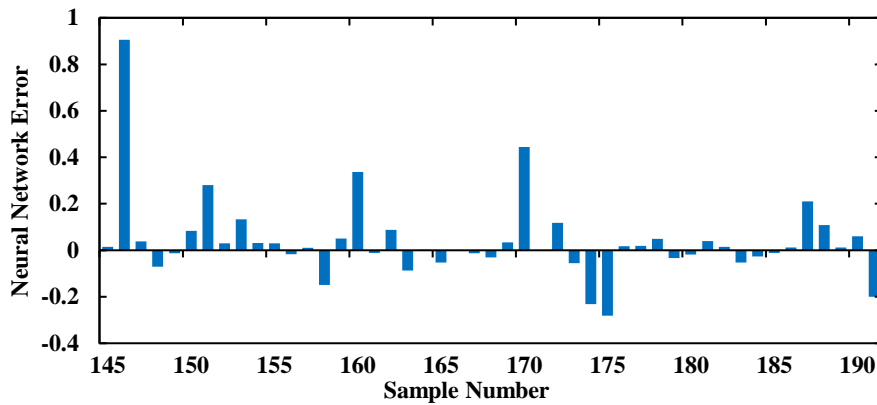


Figure 9. Error-values obtained from validation data for the hybrid wavelet and artificial neural network model

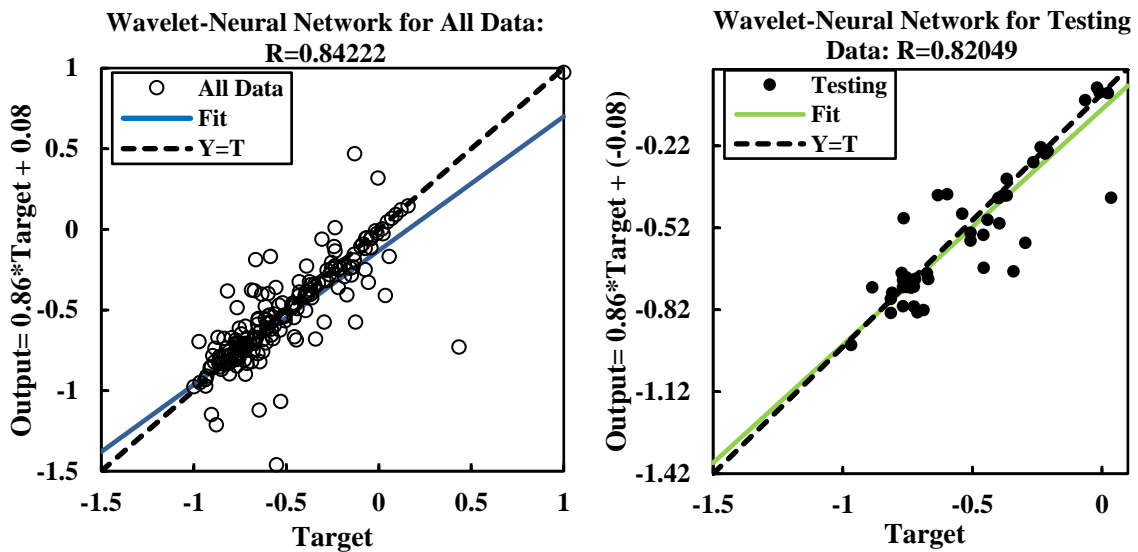


Figure 10. The correlation coefficient for validation data and whole dataset from the *dmev* wavelet-ANN combination model

Considering that the pre-processing of 5 hydraulic parameters was performed by the wavelet transform method and input to the neural network, this factor leads to accurate predictions of the final scour depth of the wavelet-neural network combination method compared to the neural network method. According to the evaluation criteria, the most accurate results combine the best effective hydraulic parameters, wavelet functions, and many neural network neurons.

4.3. Results of compilation wavelet model and ANN

In the compilation wavelet-ANN model which is obtained by replacing the standard neural network activator functions with various wavelet functions, the determination of the wavelet function, and the coefficients of scale and transmission are of great importance. By examining one or more representatives of each family of wavelet functions, a general evaluation is performed. The wavelet functions used together with the corresponding equation as an ANN activator function are presents in Table 7.

Table 7. Wavelet functions used in the compilation model [74]

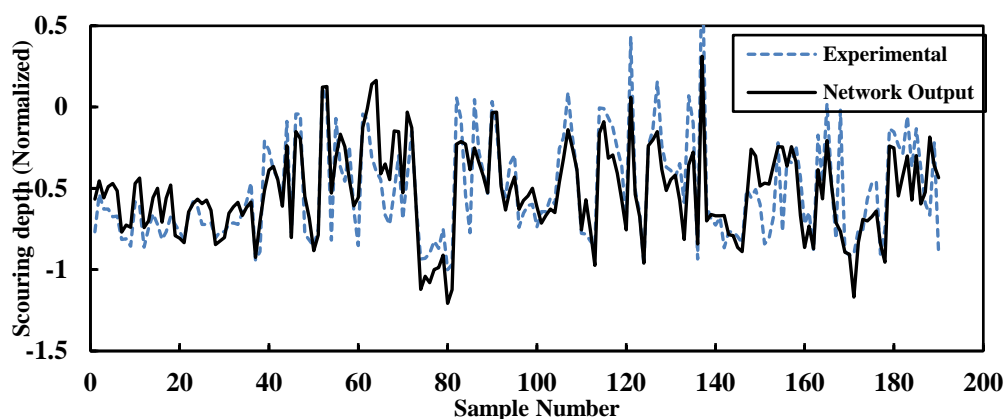
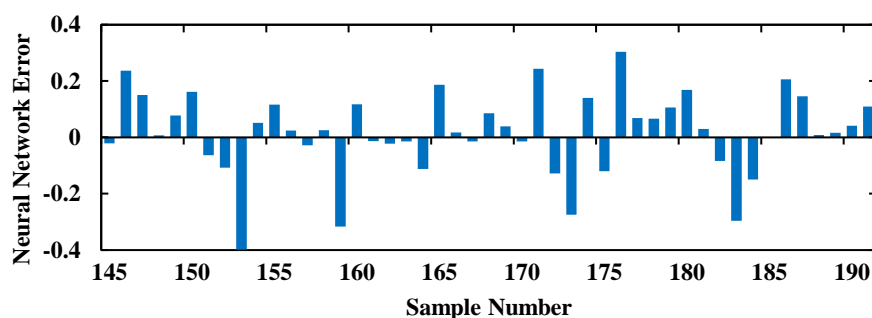
Wavelet name	Wavelet equation
Shannon	$(\sin(2\pi n) - \sin(\pi n))/(\pi n)$
Mexican Hat	$(1.5811 \left(\frac{2}{\sqrt{3}\pi^{(1/4)}} \right) e^{-(n^2/2)})(1 - n^2)$
Morlet	$e^{-(n^2/2)} \cos(5n)$
Polywog1	$\sqrt{e^1} \times n \times e^{-(n^2/2)}$
Polywog2	$0.7246 \times (n^3 - 3n) e^{-(n^2/2)}$
Polywog3	$(1/3) \times (n^4 - 6n^2 + 3) e^{-(n^2/2)}$
Polywog4	$(1 - n^2) e^{-(n^2/2)}$
Slog1	$(1/1 + e^{(-n+1)}) - (1/1 + e^{(-n+3)})$
Slog2	$(3/1 + e^{(-n+1)}) - (3/1 + e^{(-n+1)})$
Rasp1	$3.0778 \times n/(n^2 + 1)^2$
Rasp2	$2.7435 \times n \times \cos(n)/(n^2 + 1)$
Rasp3	$0.6111 \times \sin(\pi n)/(n^2 - 1)$

The results presented in Table 8 include the values of the evaluation criteria, including the correlation coefficient and the root mean square error. According to these values, it is seen that the *Polywog4* function has an excellent ability to estimate scour depth based on high correlation coefficient values and low RMSE. Figure 11 shows the overlap of experimental data and the output of the compilation wavelet and neural network model for all data. It is inferred from this that the model correctly detects the output behavior and moves in its direction but has a reasonable amount of error at the relative minima and maxima of the output signal. The error value from the *Polywog4* wavelet method and neural network with experimental observations was 1.24%.

Figure 12 is a prediction error devoted solely to data validation. As can be seen from Figure 12, a significant overlap is obtained between the model output and the experimental values, and the corresponding curves are approximately coupled. Figure 13 also compares the predicted and measured correlation coefficient, for the total and the testing datasets. The closeness of the fit to the data gives an indication of the estimation capability.

Table 8. Evaluation criteria values for combination wavelet model and artificial neural network

Wavelet name	Number of neurons	R		RMSE	
		Train	Test	Train	Test
Shannon	10	0.8318	0.8147	0.1853	0.1664
Mexican Hat	12	0.8542	0.8100	0.1656	0.1740
Morlet	12	0.7011	0.8537	0.2252	0.1679
Polywog1	11	0.7715	0.8629	0.1955	0.1828
Polywog2	12	0.8460	0.7458	0.1752	0.2279
Polywog3	10	0.7147	0.8651	0.2119	0.1936
Polywog4	9	0.7757	0.8659	0.2059	0.1457
Slog1	12	0.8685	0.8202	0.1657	0.1876
Slog2	9	0.6730	0.7400	0.2460	0.1961
Rasp1	10	0.8179	0.8643	0.1802	0.1651
Rasp2	11	0.8463	0.7714	0.1769	0.1711
Rasp3	9	0.7381	0.8800	0.2130	0.1795

**Figure 11. Overlap obtained from the *Polywog4* model and experimental data for the entire dataset****Figure 12. Error-values obtained from validation data for the *Polywog4* model**

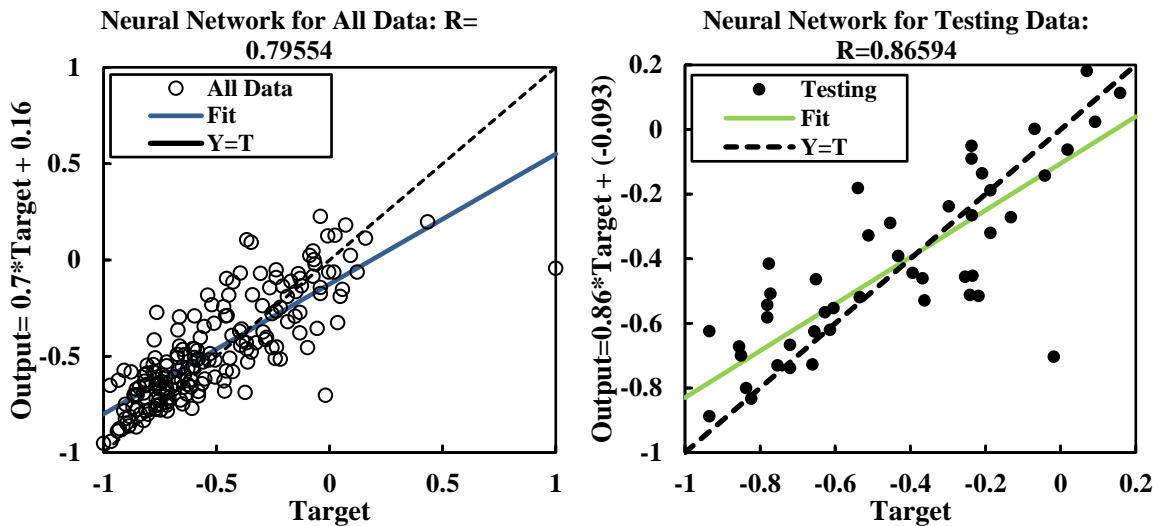


Figure 13. The correlation coefficient for validation data and whole data in *Polywog4* wavelet model compilation with ANN

In the final comparison, the values of evaluation criteria including correlation coefficient and root mean square errors are given in Table 9. The results show that the compilation of wavelet and neural network approach with the replacing the neural network activator function with the wavelet function will further improve the network. In order to better understand the effect of wavelet functions of the two methods applied, the improved values of evaluation criteria are presented. These values are obtained by dividing the absolute value of the difference between the correlation coefficient of the desired method from the neural network and the correlation coefficient of the neural network.

Table 9. Values obtained from the performance criteria of the various methods

Method	R		RMSE		Number of neurons	Percentage of improvement
	Train	Test	Train	Test		
Neural network	0.81	0.80	0.1890	0.1882	11	–
Wavenet	0.85	0.82	0.1786	0.1815	22	2.5
Wavelet - Neural Network	0.78	0.87	0.2059	0.1457	9	8.75

In the wavelet-neural network compilation method, 5 hydraulic parameters that explained in Table 3 were utilized in the wavelet-neural network compilation method with the mechanism of switching the standard neural network activator functions with various wavelet functions. This factor is the reason for the superiority of the wavelet-neural network compilation method in predicting the final scour depth compared to the neural network method and hydraulic wavelet-neural network conversion. To accurately predict the scour depth, the effective hydraulic parameters of different wavelet functions in the neural network were changed according to the evaluation criteria. Percentage of improvement compared to the first row of Table 9, which is the measure of regression improvement. The most accurate results are a compilation of the best



effective hydraulic parameters, the compilation of wavelet function and neural network, and the number of ANN neurons.

5. Conclusion

In this study, the prediction of the local scour near a cylindrical bridge pier was investigated using a compilation of the wavelet model and ANN. By examining different transmission functions, it was observed that the most suitable wavelet transmission function for separation in the structure of the wavelet-neural network to estimate local scour depth is the dmey transmission function. In the compilation wavelet-neural network method, the Polywog4 wavelet function showed a more efficient performance compared to other wavelet functions. Comparing the predictability of the wavelet-artificial neural network and compilation of the wavelet-artificial neural network method with the experimental results of the compilation of the wavelet-artificial neural network method, when the wavelet function replaces only the activator function, adaptation increases. Examining the various rules of the error back-propagation algorithm, it was observed that the Levenberh-Margaret back-propagation algorithm gives more favorable results for the combined methods of wavelet and neural network and artificial neural network. This study shows that The error in predicting the final scour depth of the dmey wavelet and neural network combination method compared with experimental observations was 1.56%, and the error value from the Polywog4 wavelet and neural network Compilation method with experimental observations was 1.24%. The neural network method with the Polywog4 wavelet activator function with 87% correlation coefficient and 8.75% improvement is more efficient than the usual neural network model. However, in the case of data filtering by wavelet and using the obtained coefficients in equipping the neural network, the correlation coefficient is 82%, which is only a 2.5% improvement to the usual neural network model. Since the mentioned methods are data-based, a certain amount of data is required to use them. In addition, the amount of data has a direct effect on the accuracy of the method and the results.

References

1. Firat, M., and Gungor, M. (2009). Generalized regression neural networks and feed forward neural networks for prediction of scour depth around bridge pier, *Advances in Engineering Software*, 40, 731-737.
2. Guven, A., Azamathulla, H.M., and Zakaria, N.A. (2009). Linear genetic programming for prediction of circular pile scour. *Journal of Ocean Engineering*, 36, 985–991.
3. Azamathulla, H.M., Ghani, A.A., Zakaria, N.A., and Aytac, G. (2010). Genetic programming to predict bridge pier scour. *Journal of Hydraulic Engineering*, 136(3), 165–169.
4. Toth, E., and Brandimarte, L. (2011). Prediction of local scour depth at bridge piers under clear-water and live-bed conditions: comparison of literature formulae and artificial neural networks, *Journal of Hydroinformatics*, 13(4), 812-824.
5. Mostaghimzadeh, E., Ashrafi, S.M., & Adib, A. (2021). Estimation of accuracy of forecast-based policies on reservoir operation using discrete wavelet transformation and ensemble learning methods. *Iranian Water Researches Journal*, 15(2), 1-15.
6. Karimae Tabarestani, M., and Zarrati, A.R. (2015). Design of riprap stone around bridge piers using empirical and neural network method, *Civil Engineering Infrastructures Journal*, 48(1), 175-188.
7. Najafzadeh, M., Barani, G.A., and Azamathulla, H.M. (2013). GMDH to predict scour depth around a pier in cohesive soils. *Applied ocean research*, 40, 35-41.

8. Chen, B.F., Wang, H.D. and Chu, C.C., (2007). Wavelet and artificial neural network analyses of tide forecasting and supplement of tides around Taiwan and South China Sea. *Ocean Engineering*, 34(16), 2161-2175.
9. Postalcioglu, S. and Becerikli, Y., (2007). Wavelet networks for nonlinear system modeling. *Neural Computing and Applications*, 16(4), 433-441.
10. Mayorga, C.R.D., Rivera, M.A.E., Velasco, L.E.R., Fernández, J.C.R. and Hernández, E.E., (2011). November. Wavelet neural network algorithms with applications in approximation signals. In *Mexican International Conference on Artificial Intelligence (374-385)*. Springer, Berlin, Heidelberg.
11. Zhong, W., and Song, Y. (2009). Wavelet neural networks model used for runoff forecast based on fuzzy C-means clustering. In *2009 2nd International Conference on Biomedical Engineering and Informatics*, 1-5. IEEE.
12. Nazaruddin, Y.Y. (2006). Wavenet based modeling of vehicle suspension system. In *IECON 2006-32nd Annual Conference on IEEE Industrial Electronics (144-149)*. IEEE.
13. Fang, Y., and Chow, T.W. (2006). Wavelets based neural network for function approximation. In *International symposium on neural networks*, 80-85. Springer, Berlin, Heidelberg.
14. Roshangar, K. (2013). Evaluation of ANFIS machine learning approach for predicting of a local scour. In: *International Conference on Civil, Transport and Environment Engineering (ICCTEE'2013) August 28-29, 2013 Penang (Malaysia)*.
15. Sarshari, E., and Mullhaupt, P. (2015). Application of artificial neural networks in assessing the equilibrium depth of local scour around bridge piers. In: *International Conference on Offshore Mechanics and Arctic Engineering*, (Vol. 56550, p. V007T06A061). American Society of Mechanical Engineers.
16. Bonakdari, H., and Ebtehaj, I. (2017). Scour depth prediction around bridge piers using neuro-fuzzy and neural network approaches. *International Journal of Civil and Environmental Engineering*, 11(6), 835-839.
17. Esmaeili-Varaki, M., Kanani, A., and Jamali, A. (2017). Prediction of scour depth around inclined bridge piers using optimized ANFIS with GA. *Journal of Hydrosciences and Environment*, 1(2), 34-45.
18. Ismail, A. (2018). Prediction of Scour Depth Around Bridge Piers Using Evolutionary Neural Network, *Journal of Mathematical Modelling in Civil Engineering*, 14(2), 26-36.
19. Sreedhara, B.M., Rao, M., and Mandal, S. (2018). Application of an evolutionary technique (PSO-SVM) and ANFIS in clear-water scour depth prediction around bridge piers, *Journal of Neural Computing and Applications*, <https://doi.org/10.1007/s00521-018-3570-6>.
20. Sadeghfam, S., Daneshfaraz, R., Khatibi, R., and Minaei, O. (2019). Experimental studies on scour of supercritical flow jets in upstream of screens and modelling scouring dimensions using artificial intelligence to combine multiple models (AIMM). *Journal of Hydroinformatics*, 21(5), 893-907.
21. Daneshfaraz, R., Aminvash, E., Ghaderi, A., Abraham, J., and Bagherzadeh, M. (2021). SVM Performance for Predicting the Effect of Horizontal Screen Diameters on the Hydraulic Parameters of a Vertical Drop. *Applied Sciences*, 11(9), 4238.
22. Ashrafi, S.M., Mostaghimzadeh, E., & Adib, A. (2020). Applying wavelet transformation and artificial neural networks to develop forecasting-based reservoir operating rule curves. *Hydrological Sciences Journal*, 65(12), 2007-2021.

- 20 M. Seifollahi, M. A. Lotfollahi-Yaghin, F. Kalateh, R. Daneshfaraz, S. Abbasi, J. P. Abraham
23. Daneshfaraz, R., Abam, M., Heidarpour, M., Abbasi, S., Seifollahi, M., and Abraham, J. (2021). The impact of cables on local scouring of bridge piers using experimental study and ANN, ANFIS algorithms. *Water Supply*. <https://doi.org/10.2166/ws.2021.215>.
 24. Ghouschi, S.J., Manjili, S., Mardani, A. and Saraji, M.K. (2021). An extended new approach for forecasting short-term wind power using modified fuzzy wavelet neural network: A case study in wind power plant. *Energy*, 223, p.120052.
 25. Anshuka, A., Buzacott, A.J., Vervoort, R.W., & van Ogtrop, F.F. (2021). Developing drought index-based forecasts for tropical climates using wavelet neural network: an application in Fiji. *Theoretical and Applied Climatology*, 143(1), 557-569.
 26. Ouma, Y.O., Cheruyot, R., & Wachera, A.N. (2021). Rainfall and runoff time-series trend analysis using LSTM recurrent neural network and wavelet neural network with satellite-based meteorological data: a case study of Nzoia hydrologic basin. *Complex & Intelligent Systems*, 1-24.
 27. El-Hady Rady, R.A. (2020). Prediction of local scour around bridge piers: artificial-intelligence-based modeling versus conventional regression methods, *Journal of Applied Water Science*, 10 (57), 1-11. <https://doi.org/10.1007/s13201-020-1140-4>.
 28. Zarbazoo Siahkali, M., Ghaderi, A. A., Bahrpeyma, A. H., Rashki, M., & Safaeian Hamzehkolaei, N. (2021). Estimating pier scour depth: Comparison of empirical formulations with ANNs, GMDH, MARS, and Kriging. *Journal of AI and Data Mining*, 9(1), 109-128.
 29. Daneshfaraz, R., Bagherzadeh, M., Esmaeeli, R., Norouzi, R., and Abraham, J. (2021). Study of the performance of support vector machine for predicting vertical drop hydraulic parameters in the presence of dual horizontal screens. *Journal of Water Supply*, 21(1), 217-231.
 30. Fuladipannah, M., & Majediasl, M. (2021). Assessment of the geometric shape of bridge pier on the scour depth using the support vector machine.
 31. Norouzi, R., Sihag, P., Daneshfaraz, R., Abraham, J., and Hasannia, V. (2021). Predicting relative energy dissipation for vertical drops equipped with a horizontal screen using soft computing techniques. *Journal of Water Supply*.
 32. Chatterjee, P. (2017). *Wavelet Analysis in Civil Engineering*. ISBN 9781138893955, Published July 26, 2017 by CRC Press, 224 Pages 90 B/W Illustrations.
 33. Adamowski, J., and Sun, K. (2010). Development of a coupled wavelet transform and neural network method for flow forecasting of non-perennial rivers in semi-arid watersheds. *Journal of Hydrology*, 390(1-2), 85-91.
 34. Coleman, N.L. (1971). Analyzing laboratory measurements of scour at cylindrical piers in sand beds. *Proc. 14th IAHR Congress, Paris, France*, 3, 307-313.
 35. Norman, V.W. (1975). Scour at selected bridge sites in Alaska. *US Geological Survey, Water Resources Division*. 75, 32-75. <https://DOI.org/10.3133/wri7532>.
 36. Jain, S.C. and Fischer, E.E. (1980). Scour around bridge piers at high flow velocities. *Journal of Hydraulic Engineering, ASCE*, 106(11), 1827-1842.
 37. Samaga, B.R. Ranga Raju, K.G. and Garde, R.J. (1985). Concentration distribution of sediment mixtures in open-channel flow. *Journal of hydraulic research*, 23(5), 467-483.
 38. G"unyakti, A. A., "Graphical Procedure for the Determination of Local Scour Around Bridge Piers", *Journal of Engineering and Environmental Sciences, Scientific and Technical Research Council Turkey*, 12(1):96-108, 1988, (in Turkish).
 39. Melville, B.W. and Sutherland, A.J. (1988). Design method for local scour at bridge piers. *Journal of Hydraulic Engineering*, 114(10), 1210-1226.



40. U.S. DOT. (1993). Evaluating scour at bridges. Hydraul. Eng. Circular No.18, FHWA-IP-90-017, Fed. Hwy. Admin., U.S. Dept. of Transp., McLean, Va.
41. Melville, B.W. and Coleman, S.E. (2000). Bridge scour. Water Resources Publication.
42. Daneshfaraz, R., Ghaderi, A., Sattariyan, M., Alinejad, B., Majedi-Asl, M., and Di Francesco, S. (2021). Investigation of local scouring around hydrodynamic and circular pile groups under the influence of river material harvesting pits. *Journal of Water*, 13(16), 2192. <https://doi.org/10.3390/w13162192>.
43. Jeng, D.S., Bateni, S.M., and Lockett, E. (2005). Neural network assessment for scour depth around bridge piers. *Civil Engineering Research Rep* (No. R855), 1-89.
44. Kothiyari, U.C. Ranga Raju, K.G. and Garde, R.J. (1992). Live-bed scour around cylindrical bridge piers. *Journal of Hydraulic Research*, 30(5), 701-715.
45. Melville, B.W. and Raudkivi, A.J. (1977). Flow characteristics in local scour at bridge piers. *Journal of Hydraulic Research*, 15(4), 373-380.
46. Chabert, J. and Engeldinger, P. (1956). Etude des affouillements autour des piles des ponts. Laboratoire d` Hydraulique, Chatou, France (in French).
47. Chee, R.K.W. (1982). Live-bed scour at bridge piers. Publication of: Auckland University, New Zealand, (290).
48. Chiew, Y. M. (1984). Local Scour at Bridge Piers. Rep No.355, School of Engineering, The Univ. of Auckland, Auckland, New Zealand.
49. Ettema, R.E. (1980). Scour at bridge piers. Rep. No. 216, Auckland, New Zealand: University of Auckland.
50. Graf, W.H. (1995). Load scour around piers. Annu. Rep., Laboratoire de Recherches. Hydrauliques, Ecole Polytechnique Federale de Lausanne, Lausanne, Switzerland, B.33.1 – B.33.8.
51. Hancu, S. (1971). Sur le calcul des affouillements locaux dans la zone des piles des ponts. Proc. 14th IAHR Congress. Paris, France, 3, 299-313.
52. Kwan, T.F. (1988). A study of abutment scour.
53. Melville, B.W. (1997). Pier and Abutment Scour – An Integrated Approach. *Journal of Hydraulic Engineering*, 123(2), 125- 136.
54. Oliveto, G. and Hager, W.H. (2001). Clear-water pier and abutment scour. In XXIX IAHR Congress Proceedings. Theme D. Hydraulics of Rivers, Water Works and Machinery (1, 7-12). Tsinghua University Press.
55. Choi, S.U. & Cheong, S. (2006). Prediction of local scour around bridge piers using artificial neural networks, *J. of the American Water Resources Association (JAWRA)*, 42, 487-494. <https://doi.org/10.1111/j.1752-1688.2006.tb03852.x>.
56. Laursen, E.M., & Toch, A. (1956). Scour around bridge piers and abutments (Vol. 4). Ames, IA: Iowa Highway Research Board.
57. Neill, C.R. (1973). Guide to bridge hydraulics. roads and transportation Assoc. of Canada, University of Toronto Press, Toronto, Canada.
58. Lee, T.L., Jeng, D.S., Zhang, G.H., Hong, J.H. (2007). Neural network modeling for estimation of scour depth around bridge piers, *J. of Hydrodynamics*, 19 :378-386.
59. Shen, H. W. (1971). Scour near piers. In: *River Mechanics*, II, Chap. 23, Ft. Collins, Colo.
60. Ettema R.E., Melville B.W., and Barkdoll, B. (1999). Closure. A scale effect in pier-scour experiments. *Journal of Hydraulic Engineering, ASCE*, 125(8), 895-896.
61. Bateni, S. M., Borghei, S. M., & Jeng, D. S. (2007). Neural network and neuro-fuzzy assessments for scour depth around bridge piers. *Engineering Applications of Artificial Intelligence*, 20(3), 401-414.

- 22 M. Seifollahi, M. A. Lotfollahi-Yaghin, F. Kalateh, R. Daneshfaraz, S. Abbasi, J. P. Abraham
62. Breusers, H.N.C., Nicollet, G., Shen, H.W. (1977). Local scour around cylindrical piers. *Journal of Hydraul Res*, 15(3), 211–52.
 63. Melville, B.W., and Chiew, Y.M. (1999). Time scale for local scour depth at bridge piers. *Journal of Hydraul Eng*, 125(1), 59–65.
 64. Ismail, A., Jeng, D.S., Zhang, L.L., and Zhang, J.S. (2013). Predictions of bridge scour: Application of a feed-forward neural network with an adaptive activation function. *Engineering Applications of Artificial Intelligence*, 26(5-6), 1540-1549.
 65. Zounemat-Kermani, M., and Teshnehlab, M. (2008). Using adaptive neuro-fuzzy inference system for hydrological time series prediction, *Applied soft computing*, 8 (2), 928-936.
 66. Salim, M., and Jones, J.S. (1980). Scour around exposed pile foundations, ASCE, *Comp. of Conf. Scour Papers (1991–1998)*, Reston, VA, 1998.
 67. Max Sheppard, D., and Glasser, T. (2004). Sediment scour at piers with complex geometries, in: *Proceedings of the 2nd International Conference on Scour and Erosion*, World Scientific, Singapore.
 68. Ataie-Ashtiani, B., Beheshti, A.A. (2006). Experimental investigation of clear-water local scour at pile groups, *J. Hydraul. Eng.*, ASCE, 132(10), 1100–1104.
 69. Farokhnia, A., and Morid, S. (2010). [Uncertainty analysis of artificial neural networks and neuro-fuzzy models in river flow forecasting](#), *Iran-Water Resources Research Journal*. 5(3), 14-27. (In Persian)
 70. Khashei, A., Shahidi, A., pourrezabilondi, M., Amirabadizadeh, M., jafarzadeh, A. (2018). [Performance Assessment of ANN and SVR for downscaling of daily rainfall in dry regions](#), *Iranian Journal of Soil and Water Research*, 49(4), 781-793. (In Persian)
 71. Lan, S., Li, S., Shahbaba, B. (2021). Scaling up bayesian uncertainty quantification for inverse problems using deep neural networks. *Arxiv preprint arxiv: 2101. 3906 (2021)*.
 72. Pourreza Bilondi, M., and Khashei-Siuki, A. (2015). [Uncertainty analysis of artificial neural networks in simulation of saturated hydraulic conductivity using Monte-Carlo simulation](#). *Iranian Journal of Irrigation and Drainage*, 9(4), 655-664. (In Persian)
 73. Dufлот, L.A., Reisenhofer, R., Tamadazte, B., Andreff, N., and Krupa, A. (2019). Wavelet and shearlet-based image representations for visual servoing. *The International Journal of Robotics Research*, 38(4), 422-450.
 74. Lekutai, G. (1997). Adaptive self-tuning neuro wavelet network controllers (Doctoral dissertation, Virginia Polytechnic Institute and State University).



© 2021 by the authors. Licensee SCU, Ahvaz, Iran. This article is an open access article distributed under the terms and conditions of the Creative Commons Attribution 4.0 International (CC BY 4.0 license) (<http://creativecommons.org/licenses/by/4.0/>).

